Ultrashort *Q*-switched pulses from a passively mode-locked distributed Bragg reflector semiconductor laser

Michael J. Strain,* Marco Zanola, G. Mezösi, and Marc Sorel

School of Engineering, University of Glasgow, Glasgow G12 8LT, UK

**Corresponding author: michael.strain@glasgow.ac.uk*

Received July 23, 2012; revised August 28, 2012; accepted September 10, 2012; posted September 11, 2012 (Doc. ID 172807); published November 14, 2012

A compact semiconductor mode-locked laser (MLL) is presented that demonstrates strong passive *Q*-switched mode-locking over a wide range of drive conditions. The *Q*-switched frequency is tunable between 1 and 4 GHz for mode-locked pulses widths around 3.5 ps. The maximum ratio of peak to average power of the pulse-train is >120, greatly exceeding that of similarly sized passively MLLs. © 2012 Optical Society of America

OCIS codes: 140.4050, 140.5960.

Semiconductor mode-locked lasers (MLLs) have been shown to exhibit ultrashort pulses with temporal durations of less than a picosecond [1] and repetition rates up to hundreds of GHz [2]. However, generating ultrashort pulses with low repetition rates in the GHz range with increased peak/average power ratios is still a major challenge, with potential applications in nonlinear optics and microscopy. Some MLL geometries have demonstrated pulse generation at GHz frequencies, including external cavity lasers, and long-cavity monolithically integrated devices. The external cavity scheme produces stable passively mode-locked ps pulse trains at low repetition rates but requires free-space cavity lengths of over 14 cm, making it unsuitable as a fully integrated solution [3]. A fully monolithic device has been demonstrated using passive/active integration and hybrid mode-locking, in order to overcome the instabilities inherent in long cavity integrated devices, to generate a 1 GHz pulse train [4]. In this case the device is still ≈4 cm long and produces pulses of a few tens of picoseconds in temporal width, with significant satellite pulses.

Alternatively, direct *Q*-switching of semiconductor lasers can produce pulse trains at hundreds of MHz repetition rates, but pulse-widths are typically in the order of 100′ s of ps [5].

The combination of these two effects, mode-locking and *Q*-switching, has been demonstrated near threshold in passively MLLs as amplitude modulation instabilities that manifest as low frequency noise on the pulse train [6]. These effects can clearly be observed in the RF spectrum and autocorrelation traces. Usually these instabilities are considered as detrimental and schemes have been presented to minimize their effects [7]. However, this *Q*-switched mode-locking behavior can be a desirable effect. If the mode-locked pulse train is fully extinguished outside of the *Q*-switching window then the pulse energy is confined to the short burst of pulses within the window, enhancing the peak/average power ratio of the device. A compact passively mode-locked Fabry–Perot (FP) laser operating in a strongly *Q*-switched regime has been proposed that can produce short bursts of mode-locked pulses at the *Q*-switched frequency, in devices of only millimeters in length [8]. Clear low frequency RF peaks have been observed in a number of works [6,8], over limited ranges of drive conditions, though full extinction of intermediate pulses in the time domain has not previously been reported for a compact monolithic device.

In this Letter, we present a passively mode-locked semiconductor laser that produces strong *Q*-switched mode-locking operation over a wide range of drive conditions. The device is based on a three-section geometry including saturable absorber (SA), gain, and distributed Bragg reflector (DBR) sections, as shown in Fig. 1. The SA length is 5% of the full cavity length with a fundamental round-trip frequency of ≈32 GH*z*. The DBR is fabricated as a sidewall relief structure of 250 μm in length and a maximum recess depth of 500 nm. In order to minimize ripples in the grating reflection spectrum the recess depth is apodized along the propagation length. The grating central wavelength is designed to have a reflection maximum around 1550 nm. Finally, the output waveguide after the DBR section is tilted and tapered to minimize back reflections to the cavity. The laser was fabricated on the AlGaInAs/InP based material system presented in [6,9] using *e*-beam lithography.

In order to characterize the operating regimes of the laser, it was mounted on a thermally controlled stage (set at 20°C), and the laser output was coupled into a lensed optical fiber. The signal was then split and simultaneously sent to a second harmonic geneneration autocorrelator, optical spectrum analyzer (OSA), and RF spectrum analyzer. Measurements were performed over a range of drive currents and voltages on the gain and SA sections, respectively. Figure 2 shows a map of the laser

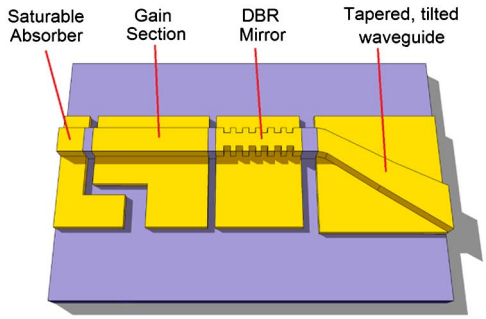

Fig. 1. (Color online) Schematic of a three-section DBR MLL.

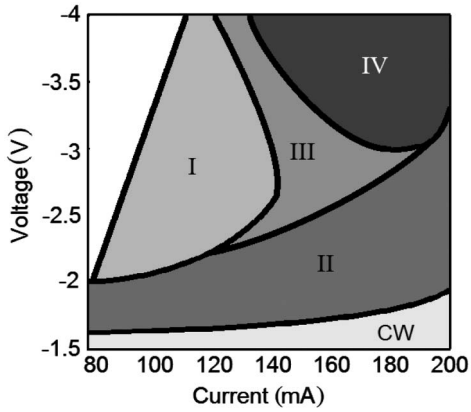

Fig. 2. (Color online) Operating regimes of a DBR MLL as a function of drive conditions. (I) Unstable mode-locking. (II) Mode-locking. (III) Mode-locking with Q-switched instabilities. (IV) Full Q-switched mode-locking.

operating regimes as function of the injection current and reverse bias on the SA, while Fig. 3 shows autocorrelation, OSA, and RF traces for the device operating in these regions.

Just above threshold, region I, the laser shows amplitude modulation around the fundamental cavity repetition rate but with a significant background in the autocorrelation trace Figs. 3(a)–(c). In region II the laser exhibits passive mode-locked behavior characterized by a strong RF peak at the round-trip frequency and a background free autocorrelation trace with low amplitude modulation. The optical spectrum shows nearly 25 dB extinction between the locked modes. The laser exhibits pulses of around 2.5–4 ps in temporal width, with spectral bandwidths of ≈1 nm typical of DBR MLL devices. In region III the laser operates in the passively mode-locked regime with low amplitude Q-switched instabilities common to semiconductor MLLs. Figure 3(g)–3(i) shows low frequency noise in the RF spectrum that corresponds to the amplitude modulation in the autocorrelation trace, though the mode-locked pulse train is never fully quenched. A suppression of the extinction ratio of the modes in the optical spectrum can also be observed on the long wavelength side of the band.

Compared with the cleaved facet FP devices in [6] the DBR MLLs show the same operating regions, but over different areas of current injection and reverse bias. The DBR forces the laser to operate at the filter central wavelength over all drive conditions, whereas the FP device lases at a wavelength set by the spectral positions of the gain peak and absorber band edge. So for a FP device the peak wavelength can shift over tens of nanometers within its mode-locked operating regime, while for the DBR MLL the wavelength changes by less than 1 nm. This forcing of the lasing wavelength by the DBR produces a significant difference in the Q-switching characteristics between the two devices. Q-switched mode-locking requires a balance between the gain in the cavity and the saturable absorption [8], both of which are strongly wavelength dependent. For the FP laser this condition is only met over a small range of drive currents and bias voltages. At the onset of lasing the gain peak is typically close to the absorber band edge, giving good absorption saturation modulation. However, as the injection current is increased, Joule heating leads to a redshift in the lasing wavelength, reducing the modulation depth of the absorption as the lasing peak detunes from the absorber band edge. This saturable absorption is still enough to produce mode-locking but the total absorption is too low to allow Q-switched mode-locking. In the case of the DBR MLL, the grating forces the lasing peak to remain constant over the injection current range, and where this is close to the absorber band-edge position, a larger range of operating conditions can produce Q-switched mode-locking. Figure 4 shows the autocorrelation, OSA, and RF traces for a DBR MLL under Q-switched mode-locking operation. The autocorrelation shows significant suppression away from the Q-switched peak, with the minimum satellite pulses showing extinction of >10 dB compared with the maximum pulse. The mode-locked pulse train is exhibited at a fundamental Q-switched frequency of 1.3 GHz, with clear higher harmonics. The measured autocorrelation was curve fitted to a train of three mode-locked pulses within the Q-switched envelope, leaving the pulse-width, and side-pulse suppression ratio as free parameters. The recovered mode-locked pulses are 3.1 ps in duration with an average output power of 0.71 mW. The peak power, calculated by normalizing the energy of the fitted pulse train to the

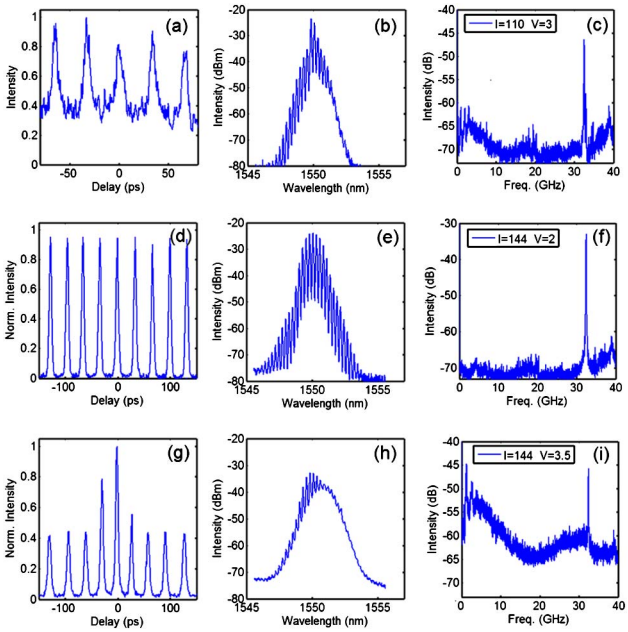

Fig. 3. (Color online) Autocorrelation traces, optical, and RF spectra for DBR MLLs operating under regions I (a)–(c), II (d)–(f), and III (g)–(i).

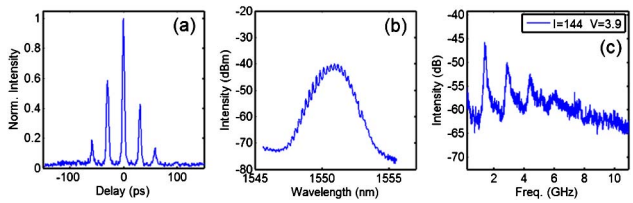

Fig. 4. (Color online) (a) Autocorrelation, (b) optical, and (c) RF spectra for a DBR MLL operating in the Q-switched mode-locking region.

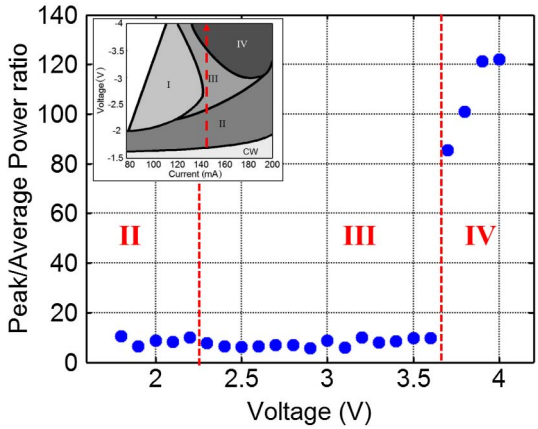

Fig. 5. (Color online) Ratio of peak to average power for a DBR MLL across operating regimes II–IV.

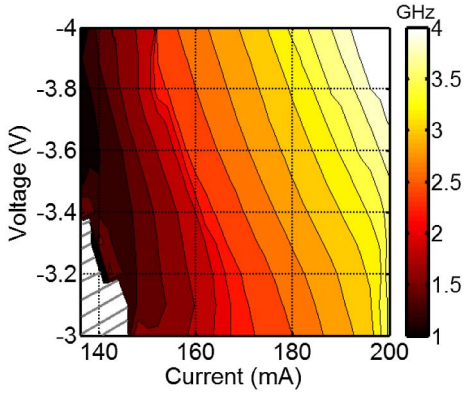

Fig. 6. (Color online) Frequency map of fundamental Q-switching frequency as a function of drive conditions. The hatched area does not exhibit full Q-switched operation.

measured average power, gives a peak pulse power of 85.9 mW for the central pulse in the burst. Figure 5 shows the peak to average power ratio of the device with varying voltage on the SA for an injection current of 144 mA. A large jump in the ratio is apparent after the transition from region III to IV in the mode-locked operation. The maximum ratio of peak power to average power is 121 for this device, significantly exceeding the typical ratio of 10 in the passively mode-locked region II.

Figure 6 shows the fundamental RF frequency of the Q-switched mode-locking as a function of drive conditions. The frequency varies between 1 and 4 GHz with low sensitivity to bias voltage on the absorber. However, by changing the injection current, the gain recovery time can be reduced, leading to an increase in the Q-switched frequency, as predicted by [8]. By varying the injection current the Q-switched frequency can be tuned by up to 47 MHz/mA for the current range shown.

In conclusion, we have presented an extremely compact passively Q-switched MLL generating ultrashort pulses at frequencies in the GHz range. The device is based on a DBR MLL geometry that employs the spectral filtering of the DBR to produce Q-switched mode-locking over a wide range of drive conditions. Peak to average power ratios of up to 121 were presented for mode-locked pulse widths of around 3.5 ps and Q-switched frequency tuning was demonstrated over a 3 GHz range.

The authors would like to acknowledge financial support from the EPSRC (project EP/E065112/1) and technical support from the staff of the James Watt Nanofabrication Centre.

References

1. Z. G. Lu, J. R. Liu, S. Raymond, P. J. Poole, P. J. Barrios, and D. Poitras, Opt. Express **16**, 14 (2008).
2. M. G. Thompson, A. R. Rae, M. Xia, R. V. Penty, and I. H. White, IEEE J. Sel. Top. Quantum Electron. **15**, 3 (2009).
3. M. J. R. Heck, E. A. J. M. Bente, B. Smalbrugge, Y. S. Oei, M. K. Smit, S. Anantathanasarn, and R. Notzel, Opt. Express **15**, 25 (2007).
4. M. G. Thompson, A. R. Rae, M. Xia, R. V. Penty, and I. H. White, IEEE J. Sel. Top. Quantum Electron. **17**, 5 (2011).
5. S. Cheung, J. H. Baek, R. P. Scott, N. K. Fontaine, F. M. Soares, X. Zhou, D. M. Baney, and S. J. Ben Yoo, IEEE Photon. Technol. Lett. **22**, 24 (2010).
6. M. B. Flynn, L. O'Faolain, and T. F. Krauss, IEEE J. Quantum Electron. **40**, 8 (2004).
7. P. M. Stolarz, J. Javaloyes, G. Mezosi, L. Hou, C. N. Ironside, M. Sorel, A. C. Bryce, and S. Balle, IEEE Photon. J. **3**, 6 (2011).
8. B. Huttl, R. Kaiser, Ch. Kindel, S. Fidorra, W. Rehbein, H. Stolpe, G. Sahin, U. Bandelow, M. Radziunas, A. Vladimirov, and H. Heidrich, Appl. Phys. Lett. **88**, 221104 (2006).
9. M. J. Strain, P. M. Stolarz, and M. Sorel, IEEE J. Quantum Electron. **47**, 4 (2011).